Tellus (1993), 45A, 289–298
Printed in Belgium – all rights reserved

TELLUS
ISSN 0280–6495

Scaling regimes of composite rainfall time series

By KLAUS FRAEDRICH* and CHRIS LARNDER,** *Meteorologisches Institut, Universität Hamburg, D-2000 Hamburg 13, Germany*

(Manuscript received 26 March 1993; in final form 21 May 1993)

ABSTRACT

The scaling behaviour of rainfall is analysed both for a range of scales in time and for a given scale in intensity using the statistics of the Fourier transform and the cumulative probability distribution. The analyses are applied to sets of long time series of daily rainfall (26 (8) files of 45 (90) years at 13 European stations) and sets of 5-min totals (13 single station summer seasons) thus covering a wide scaling range. The results of both analyses are interpreted in terms of their asymptotically hyperbolic (i.e., power law) behaviour: The ensemble averaged power spectra exhibit distinct scaling regimes with their associated power law behaviour, $P(f) \sim f^{-b}$: a regime of climatic variability (>3 years: $b \sim 0.7$), a spectral plateau (3 years to 1 month: $b \sim 0$) of general circulation fluctuations, a transition regime (1 month to 3 days: a dropping power spectrum without scaling), and a range governed by frontal systems (<3 days: $b \sim 0.5$). The transition region is interpreted as being generated by both of its neighbouring regimes whose scaling can therefore be expanded into the transition regime. Finally an apparent break in scaling (at 2.4 h) can possibly be attributed to the instruments inability to measure frequent weak signals. The tail-end of the hyperbolic distribution (characterizing the intermittency regime) is not approached smoothly but shows a break from the rest of the distribution. Finally, an outlook to multifractal scaling is given.

1. Introduction

Time scales are introduced to characterize processes which dominate the atmospheric dynamics. They are commonly identified from the spectral variance density distribution of an observed time series using the extrema and their contribution to the total variance. A famous example is the spectrum of high resolution with measurements at experimental sites (Van der Hoven, 1957; Fiedler and Panofsky, 1970; Vinnichenko, 1970). Other examples, to mention a few, are the frequency spectra deduced from daily rawin-observations at weather ships and continental stations (Hartmann, 1974), wavenumber-frequency spectra of travelling and quasi-stationary disturbances (Fraedrich and Böttger, 1978).

However, (not only the) recent progress in fractal data analysis provided some evidence that atmospheric scales may not be sufficiently defined by one or several prominent spectral peaks. On the contrary, the dynamics relevant to atmospheric phenomena may be characterized by a wide range of scales which exhibit scale invariance or scaling behaviour; that is, fluctuations at small scales are related to larger ones by the same scaling law without showing any preferred mode. Thus, the scaling behaviour within a frequency band (and not the spectral peak) may be more useful and appropriate to characterize the time scales of atmospheric dynamics. There are examples for this approach: With his "parsnip-experiment" Richardson (Ashford, 1985) applied the Lagrangian two-particle dispersion method to two-dimensional diffusion leading to his celebrated scaling law. Other examples are the Kolmogoroff 5/3-spectrum for isotropic three-dimensional turbulence, Charney's Ansatz for geostrophic turbulence, etc. More recently, in their analysis of temperatures Lovejoy and Schertzer (1986) characterize climatological regimes by

* Corresponding author.
** Department of Physics, McGill University, Montreal, Canada

scale invariance; this was extended to rainfall (Ladoy et al., 1991) with the emphasis to describe extreme variability by scaling and intermittency. Common to these analyses is the introduction of a "generalised scale invariance" which generalises the standard self-similar (isotropic) scaling approach. Thus generalised scale invariance combined with cascade models may be sufficient to describe the effect of the nonlinear scale interaction (see, for example, Lovejoy and Schertzer 1991). The traditional hydrodynamic scale analysis, however, requires the introduction of ad hoc scales and characteristic fluctuations which break the scaling. In this senses the scale analysis may be re-interpreted as an analysis of regimes which are characterized by scaling behaviour (and dynamical equations are scaling) rather than by a dominant spectral peak associated with the characteristic fluctuations.

In this paper, we apply the scaling methods to precipitation time series and identify weather and climate time scales through their scaling behaviour or scale invariance. Precipitation represents the atmosphere's input to the water (and energy) cycle modifying the radiatively forced energy budget by evaporation and thereby characterizing regional climates and climate variability. Precipitation fluctuations in time and space are due to a wide spectrum of processes which range from climate dynamics to droplet formation. This wide range of interacting scales makes it an interesting candidate for the analysis of scaling behaviour. As our main emphasis lies on the climatological re-interpretation of scales in terms of scale invariance, the discussion of the methods (Section 2) is rather elaborate, to provide a perspective for future extensions. Results are presented in Section 3; and an outlook on multifractal analysis is given in the conclusions.

2. Methods of analysis

Rainfall fluctuations cover a wide range of scales. Their variability can be analysed both for a range of scales and for a single scale: (a) *For a range of scales*, fluctuations may not display one or several prominent time scales but exhibit scale invariance (or scaling) such that fluctuations at small scales are related to larger ones by the same scaling law. (b) *For a given time scale* (minutes, days, months), fluctuations span a broad band of intensities where the (tales of the) probability distributions characterize intermittency. Both scale invariance and intermittency are statistical characteristics of the rainfall process; they can be analysed and quantified in terms of their (asymptotically) hyperbolic or power law behaviour in time which, however, is only a possibility but not automatically valid. The estimates of the related power law exponents and their range of validity define the rainfall climate, which may be associated with regions governed by the same dynamics.

2.1. *Structure function and power spectrum (Simple time scaling)*

For a *range of scales* (regimes) the second moment (variance) of a time series leads to an understanding of much of its overall variability; for multifractals, however, it leads to an understanding of the variability of a single singularity only. In the time domain a measure of the scaling behaviour of the dynamics is defined by the structure function $S(k)$ (see, for example, Monin and Yaglom, 1975) which depends on the increments of the observable $X(t)$: $X(t-k\,\Delta t)-X(t)$. Assuming a stationary process the structure function can be expressed by the auto-covariance, $B(k)$:

$$S(k) = \langle (X(t-k\,\Delta t) - X(t))^2 \rangle = 2[B(0) - B(k)], \tag{2.1}$$

where $B(0)$ is the variance of the time series, Δt the sampling time, k the time lag, and the brackets $\langle\ \rangle$ denote ensemble averaging. For self-similar scaling the structure function, $S(k)$, follows a power-law relating small time scales to small increments and vice versa. Accordingly, the Fourier-transform of the time series, $X(t)$, with such a scaling exhibits a power-law spectrum, $P(f)$:

$$S(k) = k^{2H} S(1), \qquad P(f) = Cf^{-b} \quad \text{with} \quad b = 1 + 2H, \tag{2.2}$$

where the scaling parameter $0 < H < 1$ and $C = S(1)/\pi\{\Gamma(1+2H)\sin(-\pi H)\}$ with the gamma-function Γ. Thus, regimes or dynamical scales associated with different scaling properties can now be identified by the Fourier transform (or power spectrum) of the time evolution when displayed in a log-power, $\ln P(f)$, versus log-frequency, $\ln f$, diagram.

2.2. Distributions (Hyperbolic intermittency)

At a *fixed time scale* (for example given by the sampling time), intermittency provides additional information on the variability of the intensity of the time series. An estimate is obtained from the (tale of the) probability distribution for the variate (rain), X, exceeding a fixed threshold, x:

$$F(x) = \text{Prob}\{X > x\}, \tag{2.3}$$

where $0 < F < 1$. To compare and characterize regional climates the events, $X > x$, may be normalized such that they describe their relative contribution, $R(x) = \int_x^\infty xF_x\,dx/\langle x\rangle$, to the mean, $\langle x\rangle$, where $0 \leqslant R \leqslant 1$. Eliminating x yields the cumulative probability distribution as a function of the amount, $R(x)$, which the events $X > x$ contribute to the mean. Now, interpreting F as an occupation time given by the relative number of (rain) episodes, $X > x$, (of the length of the sampling time), the following meteorologically relevant interpretation is possible: The events $X > x$, which occur in $100*F(x)$ % of the total time, contribute $100*R(x)$ % to the total rain.

Biased coin flip model and return period. Further climatologically relevant information is extracted from the probability distribution by a dichotomous analysis of the continuous rainfall variable in terms of a biased coinflip model (Gumbel, 1958). Consider observations smaller than the fixed threshold x:

$$q = 1 - F(x) = \text{Prob}\{X < x\}. \tag{2.4}$$

Then a Bernoulli experiment for the first exceedance of the threshold x at the nth trial leads to the geometric distribution, $\omega(n)$, with mean $\langle n\rangle$ and standard deviation s:

$$\omega(n) = Fq^{n-1}, \qquad \langle n\rangle = T = 1/F, \qquad s = (T^2 - T)^{1/2}. \tag{2.5}$$

Multiplied by the sampling time, the mean, $\langle n\rangle = T$, is a measure of the expected return period of (the occurrence of) an intermittent event, $X > x$, for which to happen once, $T = 1/F$ trials are necessary in the average; if x is the median, then the event $X > x$ returns on the average every second trial, $T = 2$; if x is the upper quartile: $T = 4$ etc.

Hyperbolic intermittency. Large intermittent fluctuations may be characterized by a power law (Pareto) distribution $F(x)$ with density $F_x = f$:

$$F(x) = \text{Prob}\{X > x\} = (K/x)^a,$$
$$f(x) = F_x(x) = aK^a/x^{a+1},$$

where the intermittency parameter, a, and the minimum value, K, can be estimated from quantiles of the distribution in a $\log F - \log x$ diagram. As the intermittent fluctuations show extreme variability, higher moments $\langle x^h\rangle$ of the order $h > a$ diverge as they tend to infinity for increasing sample size. Only for $h < a$ one finds (Johnson and Kotz, 1970):

$$\langle x^h\rangle = \int_K^\infty x^h F_x\,dx = aK^h/(a-h). \tag{2.6}$$

which, for example, gives the mean rainfall rate $\langle x\rangle = aK/(a-1)$. With the relative contribution to the mean, $R(x) = (K/x)^{a-1}$, one can deduce the cumulative distribution, $F = R^{a/(a-1)}$ or $R = F^{(a-1)/a}$. In this sense the hyperbolic or power law distribution characterizes intermittent behaviour by a single parameter, a, only. Here it should be mentioned that hyperbolic intermittency is the generic (but not necessary) behaviour of multifractals, hence the interest in studying it empirically. Furthermore, this power law behaviour is another type of scaling with intensity (not with spatial scale). The scale invariance is more closely related to temporal (or space) averages (say over regimes) than to fluctuations discussed in connection with the structure function. Note, however, that the assumption of an hyperbolic tail in time is quite possibly but not automatically valid.

3. Analysis of daily and 5-minute rainfall data

Daily rainfall totals from 13 continental European stations are analysed (Table 1; World Weather records until 1970, Berliner Wetterkarte from 1971). As the lengths of these time series varied from 45 to 183 years we divided the longer sets into 26 distinct separate ones of 45 years to obtain basic features of the ensemble spectrum. Then, 8 very long sets of 90 years are analysed to extend the spectrum into the ultra-long period

Table 1. *Rainfall stations used for the analysis of daily totals (and 5-min totals)*

Stations:	Years (from to)
Potsdam	1893–1986
Hohenpeissenberg	1879–1986
Frankfurt/M.	1870–1984
Uccle	1901–1986
Sonnblick	1887–1987
Geneva	1901–1985
Zurich	1901–1985
Fanoe Island	1874–1986
St. Petersburg	1881–1980
Stuttgart	1900–1976
Munich	1879–1986
Prague	1805–1988
Valentia	1939–1986
Potsdam 8 summers (May–Sept. 1975–82): 5 min totals	

range. Finally, the analysis is extended to shorter time scales using a single station time series with observations of 5 minute resolution (Potsdam, 13 summers 1975–87, from May to September). An extension to even smaller scales (1-min rainfall from Bonn and Hohenpeißenberg, one summer only) is used for qualitative arguments only (and is not shown). For the spectrum analysis we use FFT transform (Press et al., 1989) allowing for 2^n data points per file.

3.1. *Ensemble averaged spectra of daily and 5-minute rainfall*

Ensemble averages of the sample spectra of the continental European stations are presented. They are taken as averages of the amplitude of each frequency component (and then averaged over logarithmically spaced bins). Ensemble averaging has two advantages: first, the sample to sample variability of the local effects on rainfall is reduced and only dynamically relevant pattern remain. Second, the number of cycles is greatly enhanced (times the number of samples) so that the spectra may be viewed with more confidence. This is particularly so for the low frequency end of the spectrum. Note also, that the stations are not independent and the errors do not add linearly. For the very high frequency end, a single station analysis (with an ensemble of seasons) may be sufficient; our interest is only in identifying regions associated with (loosely estimated) "straight-line-regimes". Here it may be noted that the ensemble averaged spectrum of daily data of 26 files of 45 years length (Fig. 1a composed from different stations) does not deviate qualitatively from a single station ensemble mean (see Figure 2, discussed later). It exhibits several scaling regimes with the following periods: >3 years, 3 years to 1 month, 1 month to 2–3 days.

>3 years. The low frequency range (in any spectrum analysis) should be approached with care, because power estimates are based only on a small number of long period cycles. An ensemble spectrum can therefore be viewed with more confidence, because the number of cycles for the estimate is 26 times (number of the data files) better.

Towards the low frequency end the spectrum rises with decreasing frequency well outside the statistical fluctuations observed in the adjacent flat power plateau. To quantify the rise in the low frequency end, a power law behaviour, $P(f) \sim f^{-b}$, is the simplest approach giving $b = 0.7$. Deviations from a straight line can be attributed to the small number of points and the still relatively small number of cycles available for a stable estimate. The smallest period peak at 3–4 years is ambiguous whether the anomalously large amplitude with respect to the "straight line" is statistical or due to a real physical quasi-periodicity, the El Niño/Southern Oscillation, for example. Extending the ultra-long fluctuations further and to substantiate the power law governing this regime, the eight 90 year samples are averaged (Fig. 1b); they confirm the scaling behaviour. The single 180 year file has too few cycles to reveal this regime at all (not shown).

3 years to 1 month. This regime is characterized by an almost flat spectrum or spectral plateau. On this background several peaks rise which are related to intrinsic periodicities (Fig. 1c): the annual cycle, the half-annual subharmonic and a bi-annual oscillation. There is, however, another sharp but smaller peak at a period of 1.17 years, which lies above the background variation peaks. Its nature is not clear, but its period coincides with that of the Chandler Wobble (about 14 months or 1.167 years; note that the neighbouring points, at 1.18 and 1.12 years, are given by the resolution of the transform).

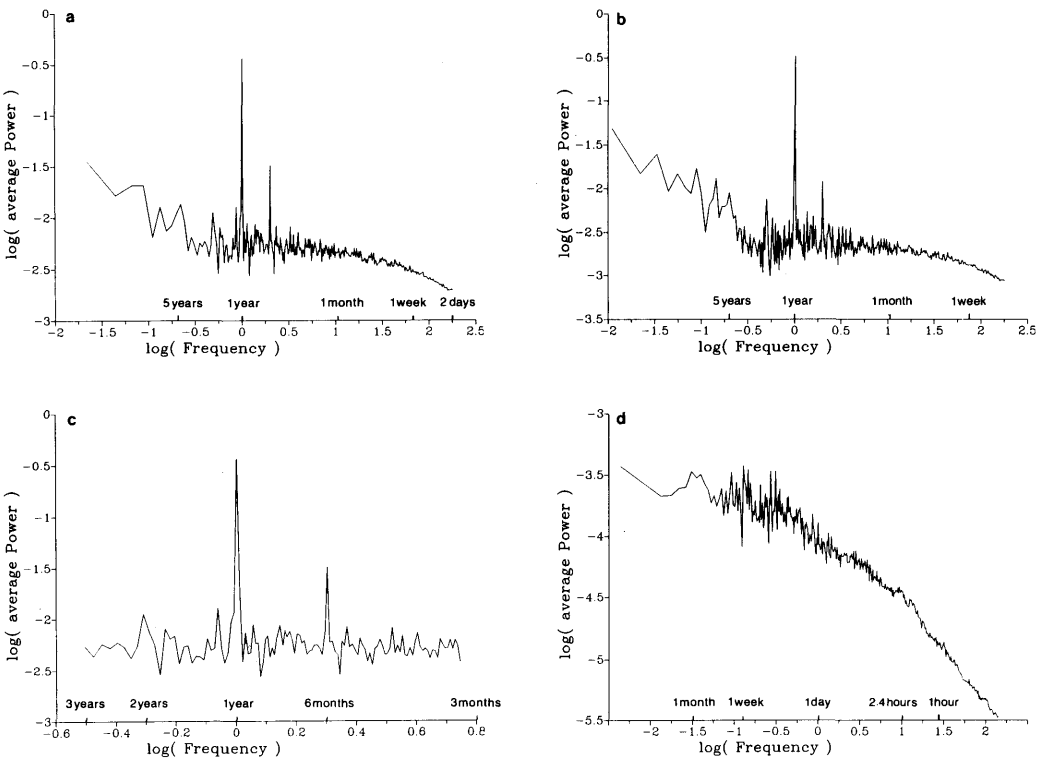

Fig. 1. Spectra of daily and 5-min rainfall totals at continental European stations: (a) Ensemble average over 26 files of 45-years, the full range of scales; (b) the low frequency part as an ensemble average over 8 files of 90 years and (c) the medium frequency part (enlarged from (a); (d) single station (Potsdam) 5-min data as the ensemble average over 8 summers (May through September), the high frequency part (note the scale change on the frequency axis). The power is averaged over logarithmically spaced bins.

1 month to 2–3 days. In this frequency range, the spectrum drops with decreasing periods, but not as a straight line in the log–log presentation (Fig. 1a). An extension towards higher frequencies and thus a clearer picture of this regime is obtained from the 5-min single station data set (13 summers from May to September in Potsdam). The season-ensemble mean shows a remarkable convergence to straight-line averages (Fig. 1d) revealing the underlying universal scaling behaviour. The regime of the dropping spectrum (1 month to 3 days) is almost fully conserved and can now be extended to the very high frequency end as follows: Commencing from longer periods (>1 month), the zero-slope near 1 month and longer confirms the flat plateau deduced from the daily data (Fig. 1c) and drops smoothly with decreasing period arriving at a slope of $b \sim 0.5$ near 2–3 days.

<3 days. The slope, $b = 0.5$, remains almost unchanged from 2–3 days to a break at the period of about 2.4 h. From 2.4 h towards the very high frequency end a new power law is attained which comes close to the famous $1/f$-noise: $P(f) \sim 1/f$ or $b \sim 1$. A first look at 1-min rainfall totals of a single summer at Hohenpeißenberg and at Bonn (based on Ombrometer measurements, Breuer and Kreuels, 1984) also revealed an almost $1/f$-power law behaviour down to scales well below 5 min.

Stability and ensemble averaging. The stability of the spectral estimates and the effect of ensemble averaging are demonstrated for a single station time series (Prague 1805–1985, Fig. 2). Noting that our interest is only in regions associated with straight-line-regimes, the following power spectral estimates of 45-year subsets of the total time series are shown: The first (a) and the last (b) subset

hardly deviate from one another in terms of the qualitative straight-line-scaling. To demonstrate that a single station scaling of the power spectral estimates does not deviate in a qualitative sense from the total ensemble presented in Fig. 1, we show (in an enlarged format with enhanced scale in the ordinate); the associated ensemble average (c) of the four 45-year files of the Prague precipitation, which is comparable with the station ensembles discussed in Fig. 1.

3.2. *Scaling regimes*

These regimes identified by the spectral analysis (Figs. 1a–d) are schematically comprised in Fig. 3; the development of a more objective method for this kind of scaling is beyond the scope of this note. The interpretation may partially be guided by the time statistics of central European fronts based on the 3-hourly synoptic sampling time and on rawinsonde spectra at European stations sampled daily (Fraedrich et al., 1979, 1986):

Climatic fluctuations (>3 years). Climate fluctuations of (relatively) short periods emerge with a power law behaviour, $P(f) \sim f^{-0.7}$, which differs from the "red noise" f^{-2}-type spectrum (Kutzbach and Bryson, 1974) which has traditionally been associated with the monoscaling Brownian motion analogue of climate fluctuations (Hasselmann, 1976) or very long term variability. The processes governing the rainfall fluctuations may follow different (and possibly more complex) climate dynamics. There is a difference between the temperature (Lovejoy and Schertzer, 1986) and the rainfall time series: The spectrum starts to "redden" from 450 years at a point to 3–5 years for northern hemisphere spatial averages, whereas the rain is reddening for point measurements near 3–5 years. Of course, to substantiate the universality of the rainfall scaling requires further analyses of very long rainfall records in other climate regions and with relatively homogeneous data sets. Finally, it should be noted that one expects time scales to be associated with the space scales of the processes. Hence we expect this scaling regime to be essentially related to variations in the whole earth's (northern hemisphere's) average.

Spectral plateau (3 years to 1 month). This regime, $P(f) \sim f^{0}$, governing the rainfall in continental Europe from about 3 years down to 3 days is basically flat except for the periodicities fixed at the annual, semi- and bi-annual cycles.

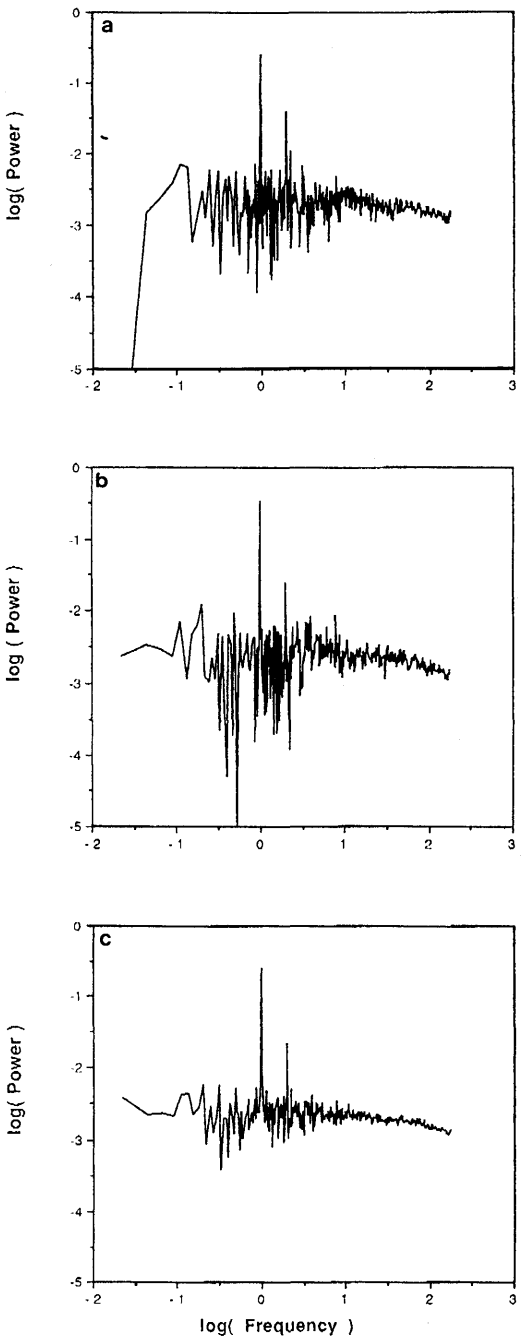

Fig. 2. Single station spectra of daily rainfall totals (Prague) of 4 consecutive 45-year subsets: (a) The first and (b) the last set; (c) the ensemble mean of all 4 subsets.

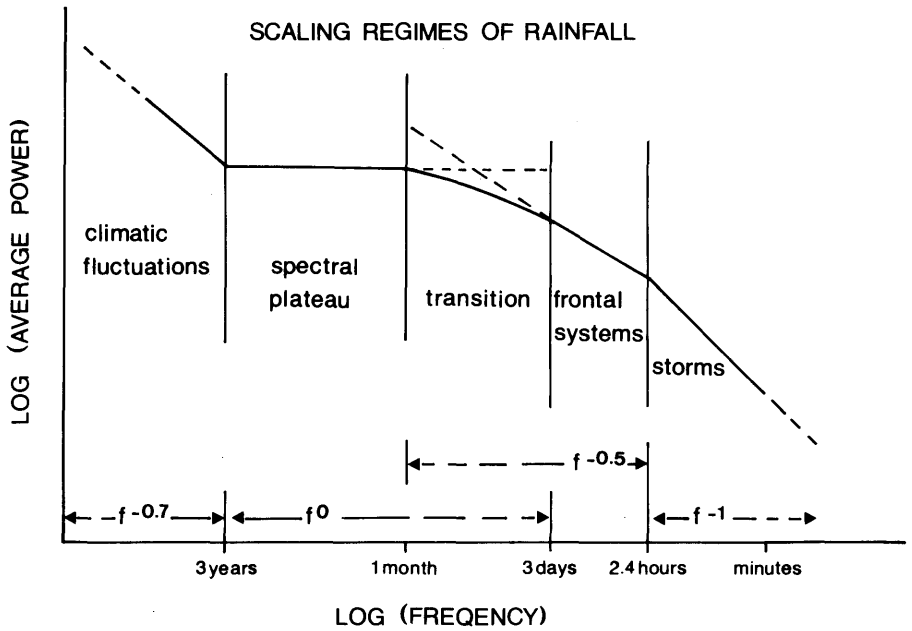

Fig. 3. Schematic diagram of the scaling regimes of continental European rainfall. The (apparent) break at 2.4 h and the standard meteorological interpretation of the associated regimes are left as open questions (see text).

This flatness, however, does not necessarily mean that the underlying process should be delta-correlated. This regime governs inter- and intra-seasonal variability. In Europe this variability can be manifested by the shifts of the sensitive tail end of the cross Atlantic storm track, the random occurrence of blocking episodes which may force (or are forced by) this shift of the cyclone track; pulses of the North Atlantic Oscillation and even far distant teleconnections with/without the influence of sea surface temperature variability, etc. Note also that the ensemble average power spectra identify a regime whose time scale limit happens to coincide with the average recurrence of one of the largest climate fluctuations on a global scale, the El Niño Oscillation (ENSO).

Transition region (1 month to 3 days). This region of a dropping spectrum appears not to be scaling (in the power law sense). It can be interpreted as a transition between two power law regimes which are both active in the same region: The flat spectrum process, $P(f) \sim f^0$ (3 years to 1 month), continues down to the period of the synoptic disturbances (about 3 days). The power law spectrum, $P(f) \sim f^{-0.5}$ (3 days to 2.4 h), is also active from 2.4 hours via 3 days to about 1 month. Thus nonlinear multiplicative interaction of these two processes effecting the rainfall can be seen as (a multiplication of the two power law straight lines leading to) the dropping in this transition or overlap region. Note that this transition region coincides with the time scales associated with the strongest synoptic scale activities (Hartmann, 1974; Speth, 1978). Plotting $fP(f)$ versus $\ln f$ (rather than $\ln P(f)$ versus $\ln f$) provides a direct measure of the variance contributed by a frequency band (= area under the $f - \ln P(f)$-graph) shows the "synoptic maximum" intensity near 20–30 days. This is the dynamics which, over Europe, is responsible for the meridional energy and momentum fluxes required to maintain the general circulation in the jet exit area of the tale end of the cross Atlantic cyclone track.

Frontal systems (< 3 days). The average duration of warm and cold fronts and occlusions lies between 8 and 12 hours and the sequence warm front-sector-cold front lasts about 29 to 34 h; modal values are shorter. Furthermore, the average recurrence time between successive cold (warm) fronts lies between 80 and 120 (230 and

Tellus A/45/4-4

105) h in summer and winter. Thus the regime, $P(f) \sim f^{-0.5}$, of frontal disturbances (carrying storms within them and clearly present from 3 days to 2.4 h) can well be extended to longer periods; that is, into the region (1 month to 3 days) of the dropping spectrum.

The break at 2–3 hours. An apparently different scaling regime occurs from 2.4 h towards the very high frequency end of the spectrum. Note that for all the above regions we were able to associate corresponding scale divisions commonly recognized in meteorology, which are associated with the predominance of one distinct physical process. Following this approach, we may identify this region as characterizing the fluctuations within the individual rain-producing meso-scale system. However, this break in scaling at 2–3 h is not generally accepted: Vinnichenko (1970) found no evidence for a meso-scale gap whereas van der Hoven's (1957) "meso-scale gap" is based on data taken under "near hurricane conditions." Therefore one has to search for sources of artificial breaks, possibly in the instrument itself. For example, the instrument's ability to measure frequent weak signals. There is a finite threshold defining the weakest signal measurable. One hypothesis is that if this threshold is too high, the small signal information loss is enough to cause the scaling to break. Indeed, first tests indicate this. Simulating an even larger threshold, the break is even stronger. Working the other way, a small enough threshold could eventually cause the break at 2.4 hour to disappear. This will be discussed in more detail in a forthcoming paper.

3.3. *Hyperbolic intermittency*

The full range of scales has been conveniently displayed by the power spectrum analyses and their ensemble averages (see above). However, this analysis is confined to the second moments (variances) and their time scaling, which needs to be extended to higher moments or, equivalently (in principle), to the complete probability distribution. In this first analysis, we have confined ourselves to the probability distribution *at a given scale* only, in order to obtain additional information about its intensity fluctuations, in particular extreme intermittency (and thus the higher moments) which is represented by the tail end of the cumulative distribution. The 5-min rainfall totals (shown in Fig. 4) reveal the following patterns. The linear drop of the tail end of the

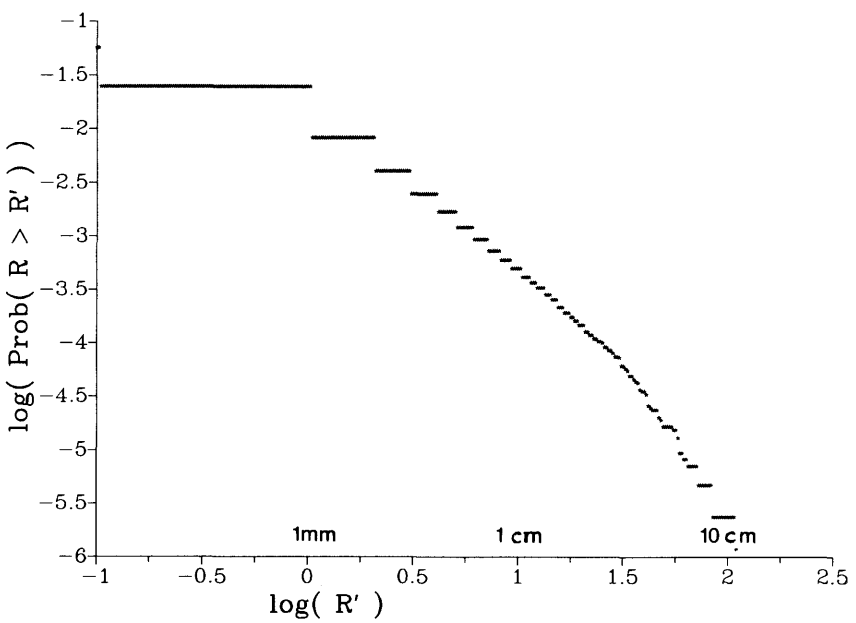

Fig. 4. Probability distribution of rainfall in a log–log diagram: Single station (Potsdam) 5-min data, distribution averaged over 8 summers.

probability distribution is not approached smoothly from the curve of the "bulk" of the distribution, but rather abruptly as a break from the rest of the distribution. Quantitatively, the tail of the distribution, if approximated by a power law of the type $F(x) = \text{Prob}\{X > x\} \sim x^{-a}$, shows a lesser reduction in probability for increasing intensity fluctuations in the 1 mm to 2 cm regime ($a \sim 1.7$), than for intensities > 2 cm ($a \sim 3.0$). That is, the recurrence time of the same hypothetically large event is shorter for the smaller slope (and vice versa). For example: an event > 10 cm, which occurs with probability 10^{-6} in the $a \sim 3.0$ regime, would, in the $a \sim 1.7$ regime, occur with probability 10^{-5} and thus return an order of magnitude earlier, a more pessimistic scenario.

4. Conclusions and outlook

The two methods of analysis demonstrated here are only a first step towards analysing stochastic nonlinear variability. Both techniques are based on a power law (or hyperbolic) behavior to quantify, in a monotonically decreasing fashion, the time and intensity structure of the rainfall signal. (1) Based on the analysis of the second moment, rainfall fluctuations are scaled in the time domain (which is equivalent to a power law structure of power spectra in the frequency domain). Thus regimes with a scaling structure can be identified and quantitatively described. (2) Using the cumulative probability distribution, the time scaling is supplemented by an amplitude scaling; an asymptotic power law behaviour of the (monotonically decreasing) intensity distribution of the signal appears to be a particularly suitable description for the occurrence of extreme events and also thus of the higher moments of the distribution. Indeed, combining both aspects (1 and 2) into the asymptotically hyperbolic distribution (and evaluating it by its moments):

$$\text{Prob}\{X > x^H\} \sim x^{-a(H)},$$

leads to the more general multifractal methods, a single description for the entire distribution at any (all) resolution(s). This spectrum of dimensions advocated by Lovejoy and Schertzer (1991) characterizes the nonlinear variability and is closely related to its (underlying) generative model of cascade processes.

5. Acknowledgements

Part of the work was supported by BMFT grant "Analyse, numerische Simulation und Vorhersage natürlicher und anthropogener Klimaänderungen" and a student research fellowship (C.L.) from McGill University, Montreal, Canada. We appreciate discussions with Drs. L. Breuer, R. Kreuels, K. Wege, S. Reich, F. W. Gerstengarbe, P. C. Werner, S. Lovejoy and D. Schertzer. The referees' comments are gratefully acknowledged, all of which contributed to a substantial improvement of the analysis.

REFERENCES

Ashford, O. M. 1985. *Prophet or Professor? The life and work of Lewis Fry Richardson.* Adam Hilger Ltd., Bristol, UK (Consultant Editor: A. J. Meadows), 304 pp.

Berliner Wetterkarte 1952–1989. Tägliche Wetterkarte (daily weather map); Nordhemisphärischer Klimabericht. Institut für Meteorologie, Freie Universität Berlin.

Breuer, L. and Kreuels, R. 1984. Dependence of rain intensity maxima on time base. *Beitr. Phys. Atmosph. 57*, 39–54.

Fiedler, F. and Panofsky, H. A. 1970. Atmospheric scales and spectral gaps. *Bull. Amer. Meteor. Soc. 51*, 1114–1119.

Fraedrich, K. and Böttger, H. 1978. A wavenumber-frequency analysis of the 500 mb geopotential at 50° N, *J. Atmos. Sci. 35*, 745–750.

Fraedrich, K., Böttger, H. and Dümmel, T. 1979. Evidence of short, long and ultra-long period fluctuations in Berlin rawinsonde data. *Contr. Atmos. Phys. 52*, 348–361.

Fraedrich, K., Bach, R. and Naujokat, G. 1986. Single station climatology of central European fronts: number, time and precipitation statistics. *Contr. Atmos. Physics 59*, 54–65.

Gumbel, E. J. 1958. *Statistics of extremes.* Columbia University Press, 375 pp.

Hartmann, D. 1974. Time spectral analysis of mid-

latitude disturbances. *Mon. Wea. Rev. 102*, 348–362; Corrigendum: 541–542.

Hasselmann, K. 1976. Stochastic climate models. *Tellus 28*, 473–485.

Johnson, N. L. and Kotz, S. 1970. *Continuous univariate distributions (I)*. John Wiley & Sons, 300 pp.

Kutzbach, J. E. and Bryson, R. A. 1974. Variance spectrum of holocene climatic fluctuations in the North Atlantic sector. *J. Atmos. Sci. 31*, 1958–1963.

Ladoy, P., Lovejoy, S. and Schertzer, D. 1991. Extreme variability of climatological data: scaling and intermittency. In: *Nonlinear variability in geophysics* (eds. S. Lovejoy and D. Schertzer). Kluwer Acad. Publishers, 241–250.

Lovejoy, S. and Schertzer, D. 1986. Scale invariance in climatological temperatures and the local spectral plateau. *Annales Geophysicae 86B*, 401–409.

Lovejoy, S. and Schertzer, D. (eds.), 1991. *Nonlinear variability in geophysics: scaling and fractals.* Kluwer Acad. Publishers, 318 pp.

Monin, A. S. and Yaglom, A. M. 1975. *Statistical fluid mechanics*, vol. 2. MIT Press, 874 pp.

Press, W. H., Flannery, B. P., Teukolsky, S. A. and Vetterling, W. T. 1989. *Numerical recipes.* Cambridge University Press, 702 pp.

Speth, P. 1978. Time-spectral analysis of large scale eddy transport of sensible heat and momentum. *Contr. Atmos. Phys. 51*, 153–165.

Van der Hoven, I. 1957. Power spectrum of the horizontal wind speed in the frequency range from 0.0007 to 900 cycles per hour. *J. Meteor. 14*, 160–164.

Vinnichenko, N. K. 1970. The kinetic energy spectrum in the free atmosphere, 1 second to 5 years. *Tellus 22*, 160–164.

Voss, R. F. 1988. Fractals in nature: From characterization to simulation. In: *The science of fractal images* (eds. H.-O. Peitgen and D. Saupe), Springer Verlag, 21–70.

World Weather Records 1944 (1881–1920), 1921–1930) and 1947 (1931–1940), Smithonian Miscallaneous Collections 1959, 79, 90, 105 (1941–1950); US Weather Bureau 1966 (1951–1960), and 1979 (1961–1970).